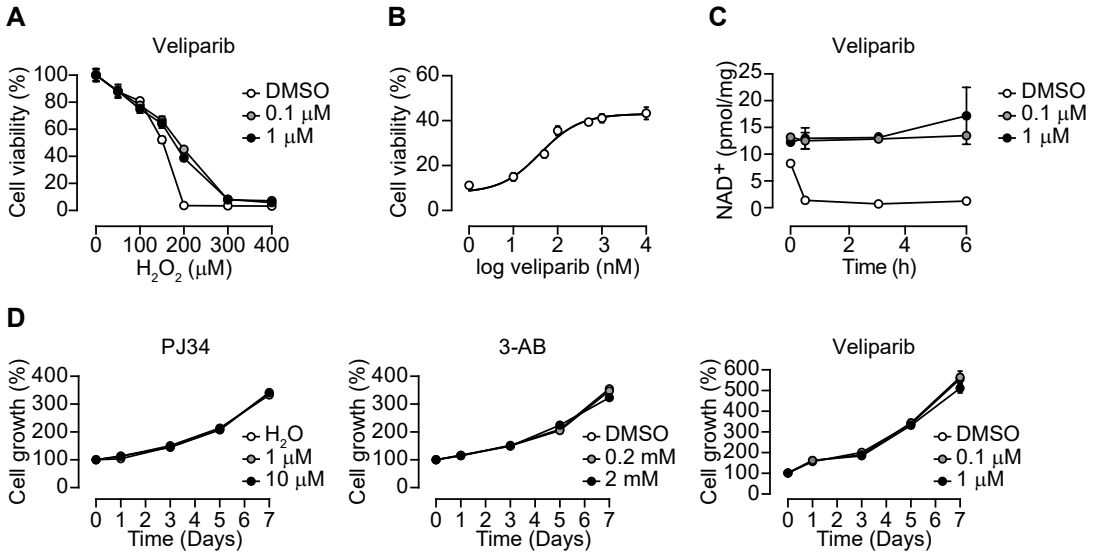

Supplemental Figure 1. PARP inhibitors prevent H_2O_2-induced cytotoxicity but do not alter proliferation of patient fibroblasts

(A) H_2O_2-induced cytotoxicity. Patient fibroblasts were treated with 0.1 and 1 μM veliparib for 1 h before a 24-h exposure to the indicated concentrations of H_2O_2. Data are means ± S.E.M. of values obtained from three experiments conducted in triplicate.

(B) Concentration-dependent effect of veliparib on H_2O_2-induced cytotoxicity. Patient fibroblasts were exposed to the indicated concentrations of veliparib for 1 h before a 24-h exposure to 200 μM H_2O_2. Cell viability was calculated by comparison to the control group (100%; cell viability without H_2O_2). Data represent means ± S.E.M. of values obtained from three experiments conducted in triplicate and were fitted to a sigmoidal (variable slope) curve. The IC_{50} of veliparib was 35.83 ± 1.25 nM.

(C) Effect of veliparib, a PARP inhibitor, on NAD^+ content after H_2O_2-induced PAR accumulation. NAD^+ concentration (pmol/μg) was measured by HPLC and normalized to protein concentration. Patient fibroblasts were incubated with Veliparib (0.1 and 1.0 μM) for 1 h before H_2O_2 (300 μM) exposure. Data are means ± S.E.M. of values obtained from two experiments. Significant differences were observed at all-time points. *$P < 0.05$.

(D) Proliferation of patient fibroblasts in the absence or presence of PARP inhibitors (i.e., PJ34, 3-AB, and veliparib) was assessed by using the CCK-8 kit. Data represent means ± S.E.M. of values obtained from three experiments conducted in triplicate.

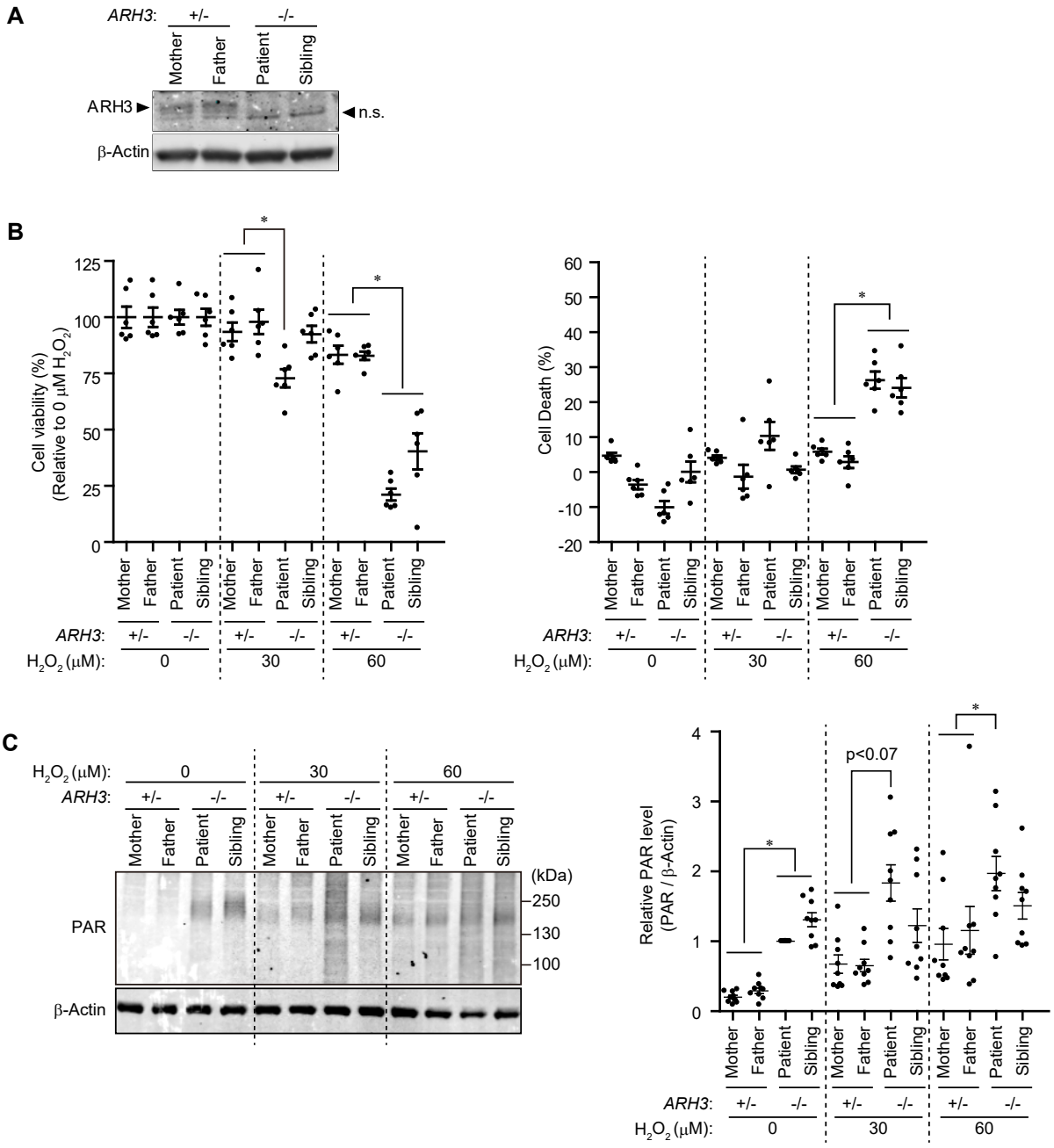

Supplemental Figure 2. Response of fibroblasts from patient and his family to H_2O_2

(A) Wild-type ARH3 protein is expressed in the mother's and father's, but not patient and the mildly affected sibling's fibroblasts. β-actin was used as a loading control. Western blots were performed with anti-ARH3 antibody recognizing the C-terminus and anti-β-actin antibody. These representative data were replicated three times with similar results.

(B) H_2O_2-induced cytotoxicity. Fibroblasts were treated with 0, 30, or 60 μM H_2O_2 for 24 h. Cell viability (left) and cell death (right) were assayed. Data are means ± S.E.M. of values obtained from two experiments conducted in triplicate. *$P < 0.05$

(C) H_2O_2-induced PAR accumulation. Fibroblasts were treated with 0, 30, or 60 μM H_2O_2 for 20 min and subjected to Western blotting with anti-PAR and anti-β-Actin antibodies. Data are means ± S.E.M. of values obtained from two experiments conducted in triplicate. *$P < 0.05$

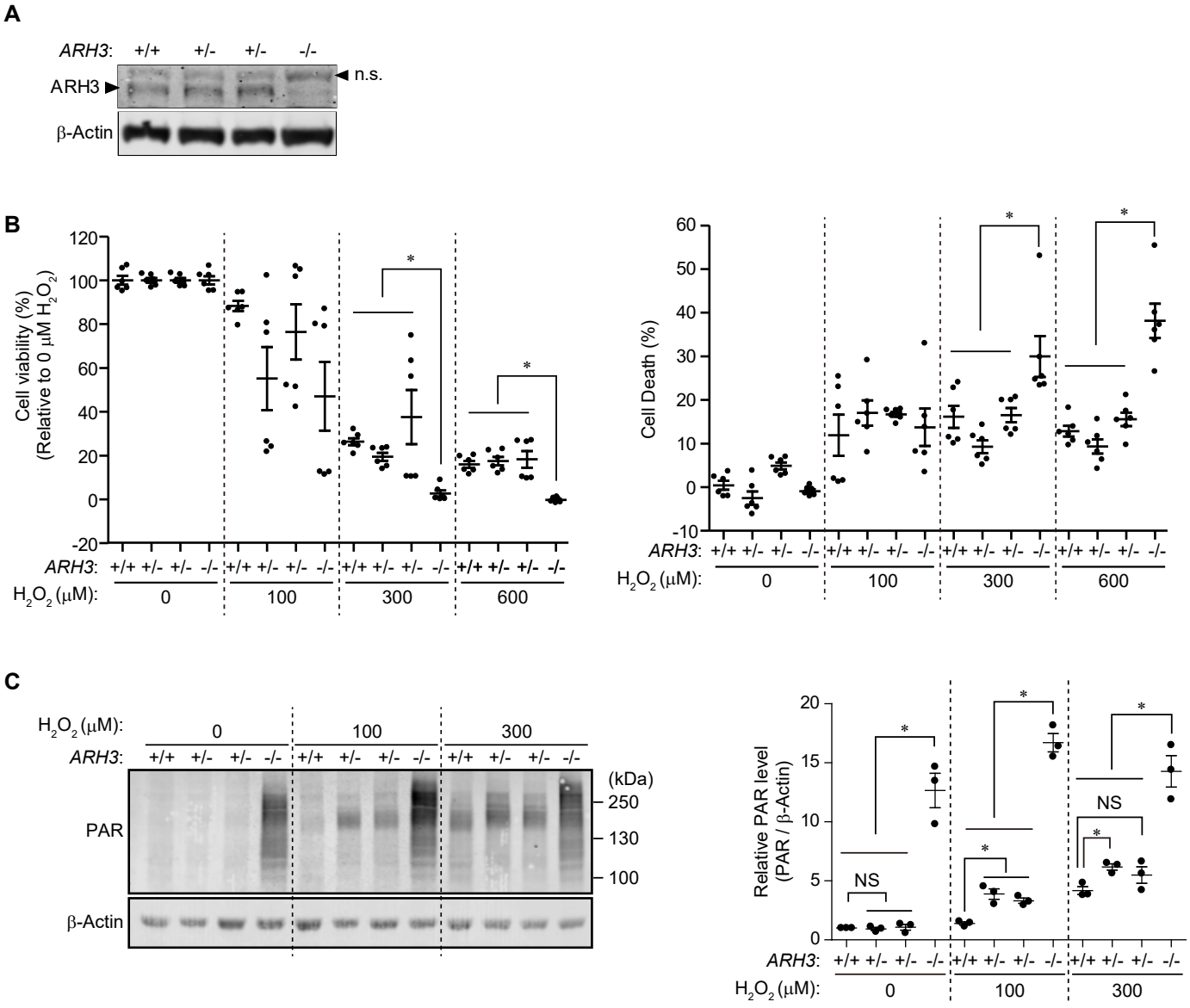

Supplemental Figure 3. Response of WT, *ARH3*$^{+/-}$ and *ARH3*$^{-/-}$ MEFs to H_2O_2

(A) ARH3 protein is expressed in WT and two cell lines of *ARH3*$^{+/-}$, but not *ARH3*$^{-/-}$ MEFs. β-actin was used as a loading control.

(B) H_2O_2-induced cytotoxicity in MEFs. MEFs were treated with 0, 100, 300, or 600 μM H_2O_2 for 24 h. Cell viability (left) and cell death (right) were assayed. Data are means ± S.E.M. of values obtained from two experiments conducted in triplicate. *$P < 0.05$.

(C) H_2O_2-induced PAR accumulation in MEFs. MEFs were treated with 0, 100, 300, or 600 μM H_2O_2 for 20 min and subjected to Western blotting with anti-PAR and anti-β-actin antibodies. Data are representative of two experiments conducted in triplicate. *$P < 0.05$, NS, not significant.

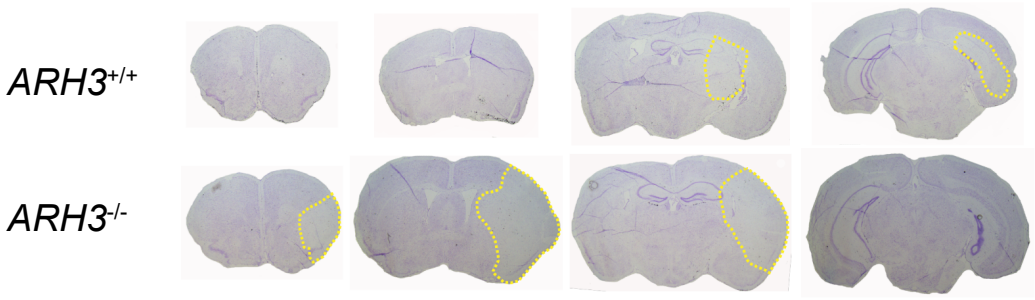

Supplemental Figure 4. Infarct brain area stained with Nissl in WT and *ARH3*$^{-/-}$ mice

Representative Nissl-stained coronal sections show infarct area (yellow dotted lines) of WT and *ARH3*$^{-/-}$ mice subjected to 30-min ischemia, followed by a 24-h reperfusion.

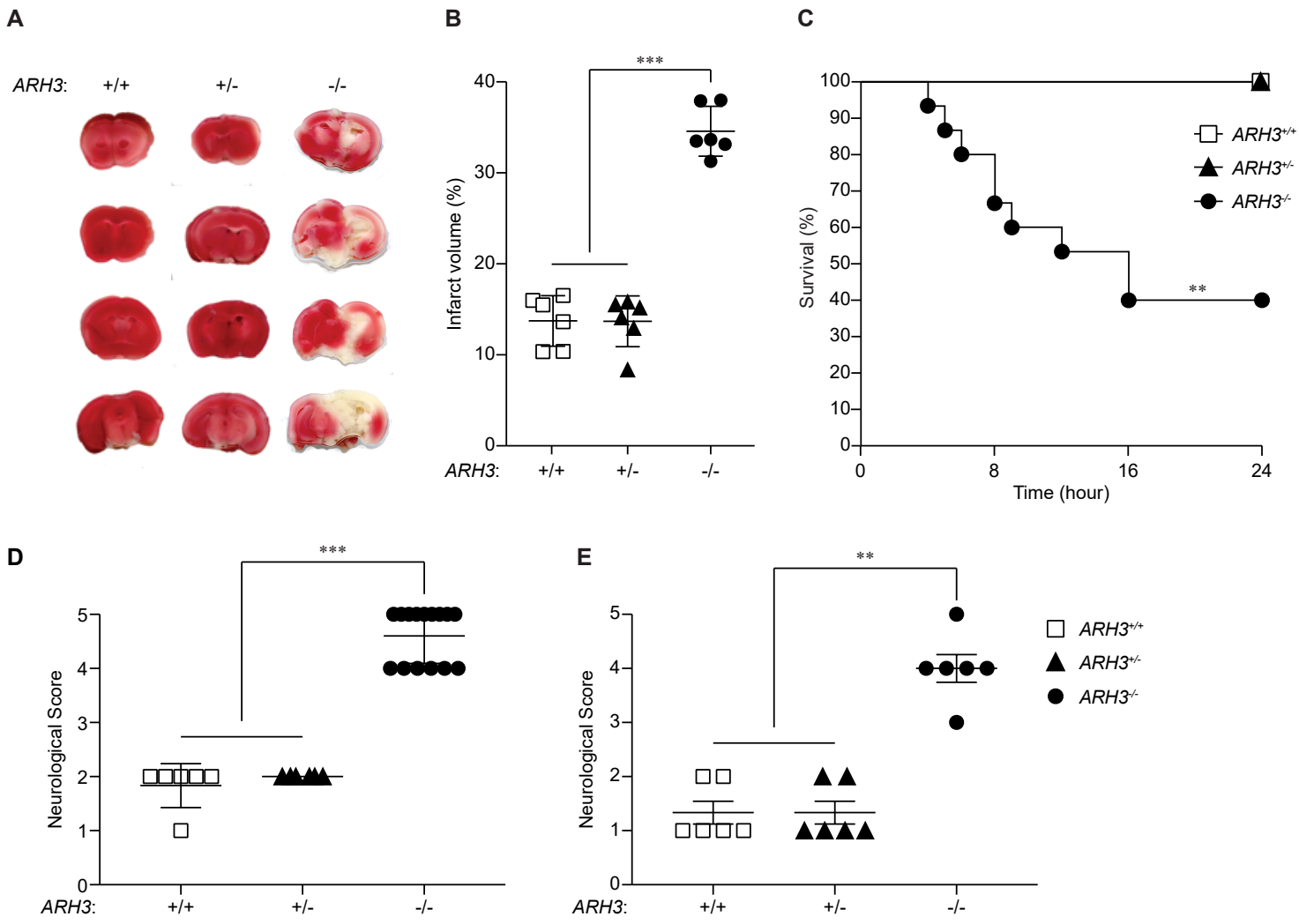

Supplemental Figure 5. Effects of *ARH3* genotype on infarct size after 30-min ischemia, followed by reperfusion.

(A) Representative coronal brain sections (2-mm thick) using TTC staining in WT, *ARH3*$^{+/-}$ and *ARH3*$^{-/-}$ mice are shown, with the infarct area, after 30-min ischemia, followed by a 24-h reperfusion. TTC staining visualizes the infarct area.

(B) Quantification of infarct size (%, infarct area vs whole brain area) was significantly greater in *ARH3*$^{-/-}$ compared with WT and *ARH3*$^{+/-}$ mice. Data are means ± S.E.M. of values obtained from 6 mice in each genotype. ***$P < 0.001$

(C) Survival rate (%) after cerebral ischemia/reperfusion of each *ARH3* genotype is shown. Survival rate in ARH3-/- mice (40% survival rate, 6 out of 15 mice) was significantly lower than that of both WT and *ARH3*$^{+/-}$ mice (100%, 6 out of 6 mice). **$P < 0.01$.

(D) Neurological deficit scores after 30-min ischemia, followed by a 1-h reperfusion, in WT, *ARH3*$^{+/-}$ and *ARH3*$^{-/-}$ mice. Data are means ± S.E.M. of values obtained from WT (n = 6), *ARH3*$^{+/-}$ (n = 6) and *ARH3*$^{-/-}$ (n = 15) and mice. ***$P <$ 0.001.

(E) Neurological deficit scores after 30-min ischemia, followed by a 24-h reperfusion, in WT, *ARH3*$^{+/-}$ and *ARH3*$^{-/-}$ mice. Nine *ARH3*$^{-/-}$ mice were dead after 24 h reperfusion. Data are means ± S.E.M. of values obtained from 6 mice in each genotype. **$P < 0.01$.

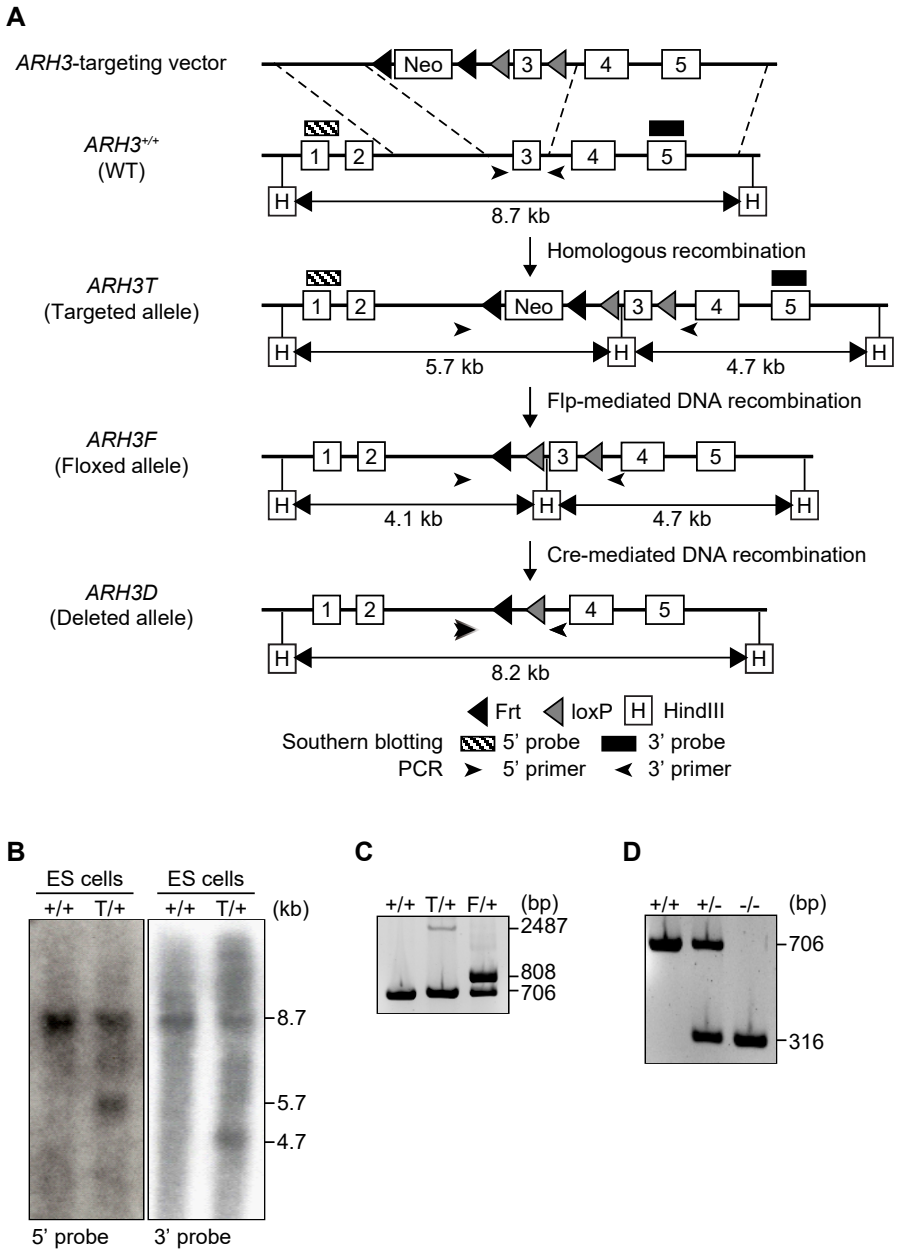

Supplemental Figure 6. Targeting of *ARH3* gene

(A) Schematic representation of targeting strategy. The neomycin resistance cassette (Neo) was flanked by Frt sites, and the exon 3 region to be deleted was flanked by loxP sites. Neo was then removed by crossing the targeted mice ($ARH3^{T/+}$) with transgenic mice expressing Flp under the control of the actin promoter (ACTB-Flp), generating the floxed allele *ARH3F*. To delete the exon 3, $ARH3^{T/+}$ mice were mated with EIIa-Cre transgenic mice ubiquitously expressing Cre recombinase.

(B) Genotyping by Southern blot analysis of ES cells after homologous recombination. Genomic DNA obtained from ES cells was digested with HindIII, subjected to electrophoresis in 1.0% agarose gel and transferred to nylon membranes. WT and targeted alleles; 8.7- and 5.7-kb bands by 5′ probe, and 8.7- and 4.7-kb bands by 3' probe, respectively.

(C, D) Genotyping of mouse embryos by PCR. These primers amplified a 2487 bp, *ARH3T* allele (T/+); 808 bp, *ARH3F* allele (F/+); 706 bp, ARH3 WT allele; 316 bp, *ARH3D*. +/+, *ARH3* WT; +/-, *ARH3* heterozygous; -/-, ARH3 homozygous.

Supplemental Table 1 Clinical information on proband

Admission	8-year-old Hispanic male, with progressive upper limb girdle neuropathy and severe muscle wasting moving distal to proximal with autonomic symptoms, dystonic torticollis and anorexia.
Onset of the disease	Freezing, increased clumsiness and decreased hand use were noted at the age of 18 months. Language skills were delayed. Received comprehensive early intervention services including Speech, OT, PT, and the assistance of a one-to-one aide at school.
Family history	The youngest and the only male of four siblings, of non-consanguineous parents. Two older female siblings died of progressive respiratory failure with the same neurodegenerative phenotype. One older sister was mild affected.
Laboratory test	Mildly elevated pyruvate at 1.9 (0.7-1.4 mg/dl). CBC, iron indices, vitamin D and carnitine levels, leukocyte CoQ levels, CK, uric acid, lactate, plasma and urine amino acids, very long chain fatty acids with pristanic and phytanic acids, N-glycan profiles, lysosomal screening panel, urine organic acids, urine oligosaccharides and mucopolysaccharides were all normal.
MRI/MRS	Brain MRI/MRS demonstrated non-specific abnormalities in the cerebellum. Total spine MRI was normal.
NCV/EMG	Revealed a severe motor neuropathy affecting the upper and lower extremities with relatively preserved sensory nerve function; a subsequent sural nerve biopsy was non-diagnostic.
EEG, EKG, Echocardiogram	Normal.
Neuropsychology	Neuropsychological testing identified poor performance in all domains including memory, math, and reading.
Others	Pulmonary function tests were consistent with mild restrictive lung disease. Eye exam revealed mild myopia with retinal pigmentary variation that was considered normal, with no optic nerve abnormalities.

Supplemental Table 2 Pathological report of proband's affected sibling

Brain	Finding
Spinal cord	Neuronal loss, gliosis and tract degeneration in the upper cervical cord
Medulla	Severe neuronal loss and gliosis in the inferior olivary, hilum and amiculum. Tract degeneration in the medial lemniscus. The pyramids and the hypoglossal nuclei appear intact, while the vestibular nuclei and dob rsal vagal nuclei are severely depleted and gliotic.
Pons	The Abducens and Facial nuclei appeared intact, as well as Locus ceruleus. Transverse fibers and descending tracts are normally present.
Midbrain	The substantia nigra is well populated. Cerebral peduncles red nuclei and oculomotor nuclei are unremarkable. The inferior colliculus shows a prominent reactive trocytosis.
Hippocampus	Extensive neuronal loss from Ammon's horn pyramidal tiectors CA 1,3,4 contrasting with relative preservation of CA2. The dentate fascia is severely depleted, and astrogliosis pervades the endplate and affected cell layers.
Cerebellum	Severely and globally affected both in the vermis and cerebellar hemisphere: considerable loss of Purkinje cells from individual cells picked off to short stretches of complete loss; granule cell depletion parallels this, and there is widespread proliferation of Bergmann glia; most striking are the innumerable eosinophilic Purkinje proximal axon swellings or torpedoes; the basket cells and their plexus which appear relatively preserved such that empty and collapsed baskets are noted where Purkinje cells have dropped out; the central white matter is patchily attenuated and gliotic; the dentate itself is severely involved and around with scattered foamy macrophages; neuronal loss is subtotal in many places with a severe astrogliosis; the hilum is gliotic and its outflow through the superior cerebellar peduncle is attenuated and gliotic.
Basal ganglia	Neuronal loss and astrocytosis in the caudate, putamen and the striatal cellular bridges. Pencil fibers remain. The subthalamic nucleus is intact.
Thalamus	Considerable neuronal loss and gliosis

Supplemental Table 3 Nucleotide primers and probes

Primer/probe	Sequence (5' to 3')
Southern blotting	
5' probe (exon 1)	Forward 5'-CGATGCCGGAAGTGGCGACTAG-3'
	Reverse
	5'-CTCTTCAAGAAGAACCAAGTCTTCTACTGACA-3'
3' probe (exon 5)	Forward 5'-AATGGCATTGCCGCCTTTGAATC-3'
	Reverse 5'-GGTCTGACAAGCCCACCGAAG-3
Genotyping PCR	
ARH3	Forward 5'-GGAAGGGAGTGGAAAGTTTCCC-3'
	Reverse 5'-AAGAGAAGGGAGGCAGATGAGAGTTT-3'
Reverse transcription-PCR	
ARH3	Forward 5'-TGGACATGGCTCACAGATTTG-3
	Reverse 5'-GCAGCGTAGGAAGCAGTAGATG-3'
Mutagenesis	
ARH3	Forward
	5'-ACAAGAAAGACCCTGACGGGCTATGGTGCTGGAG-3'
	Reverse
	5'-CTCCAGCACCATAGCCCGTCAGGGTCTTTCTTGT-3'